

Biochemical and physical investigations on detoxification of ginkgo kernel juice using probiotic fermentation with macroporous resin addition

Yuyu Sun^{1,2}, Jiaying Zhao¹, Sivakumar Manickam³, Jingyang He¹, Dandan Li¹, Yongbin Han¹, Xiaosan Jiang⁴ and Yang Tao^{1*}

¹ College of Food Science and Technology, Whole Grain Food Engineering Research Center, Nanjing Agricultural University, Nanjing 210095, Jiangsu, China

² Jinan Fruit Research Institute, All-China Federation of Supply and Marketing Co-operatives, Jinan 250220, Shandong, China

³ Department of Petroleum and Chemical Engineering, Faculty of Engineering, Universiti Teknologi Brunei, Bandar Seri Begawan BE1410, Brunei Darussalam

⁴ Taizhou Institute of Nanjing Agricultural University, Taizhou 225300, Jiangsu, China

* Corresponding author, E-mail: yang.tao@njau.edu.cn

Abstract

The toxicity of ginkgo kernel is a global concern, restricting its consumption as a medicinal food. This study focuses on eliminating the toxic components, specifically ginkgolic acid, from ginkgo kernel juice. The approach used was probiotic fermentation with autochthonous lactic acid bacteria combined with macroporous resin. Compared to using lactic acid fermentation alone, adding macroporous resin during probiotic fermentation significantly enhanced the removal of toxic ginkgolic acid and 4'-O-methylpyridoxine from ginkgo kernel juice. After 48 h of fermentation with macroporous resin, the contents of ginkgolic acid and 4'-O-methylpyridoxine decreased by more than 69% and 61%, respectively. Interestingly, the adsorption of microbial growth inhibitors, such as ginkgolic acid, 4'-O-methylpyridoxine, and phenolics, by the resin did not hinder the growth of lactic acid bacteria or their metabolic activities involving organic acids and monosaccharides. The study further confirmed that microbial adsorption was the primary reason for removing ginkgolic acid during probiotic fermentation. Also, the adsorption mechanism of ginkgolic acid during probiotic fermentation with macroporous resin was explored. From a mass transfer perspective, incorporating macroporous resin during the probiotic fermentation of ginkgo kernel juice reduced the mass transfer resistance for surface diffusion. Consequently, this lowered the contribution of surface diffusion to the overall diffusion process and facilitated the efficient removal of toxic ginkgolic acid. This work can help to understand the physical mechanism regarding detoxification of ginkgo kernel juice by probiotic fermentation, and offer potential strategies to enhance the safety of ginkgo kernel products.

Citation: Sun Y, Zhao J, Manickam S, He J, Li D, et al. 2023. Biochemical and physical investigations on detoxification of ginkgo kernel juice using probiotic fermentation with macroporous resin addition. *Food Innovation and Advances* 2(4):324–339 <https://doi.org/10.48130/FIA-2023-0032>

Introduction

The *Ginkgo biloba* tree, often called a 'living fossil', has existed on Earth for approximately 200 million years^[1]. The edible part of the fruits from the female *Ginkgo biloba* tree, known as the ginkgo kernel, holds significant nutritional and medicinal value. Numerous clinical studies have demonstrated that consuming ginkgo kernels can be beneficial in treating cardiovascular and cerebrovascular diseases, improving memory in Alzheimer's disease treatment, and promoting blood vessel health^[2,3]. However, the presence of toxins such as ginkgolic acid, 4'-O-methylpyridoxine, hydrocyanic acid, and allergenic proteins in ginkgo kernel has led to concerns among consumers regarding their safety^[4,5]. Scientific evidence indicates that consuming ginkgo kernels, especially at high doses, can have adverse effects on human health, including vomiting, seizures, skin ulceration, dyspepsia, loss of consciousness, and even death^[6–8]. To make ginkgo kernels safer and palatable, various methods, such as steaming, roasting, germination, and frying, have been explored to reduce their toxic components^[9–11].

In contrast to thermal treatments, probiotic fermentation offers a promising and innovative approach to decrease ginkgo

kernels' toxic components. Our previous research showed that fermenting ginkgo kernel juice with commercial strains of *Lactobacillus acidophilus*, *Lactobacillus plantarum*, and *Lactobacillus casei* led to a significant reduction of toxic ginkgolic acids by at least 50%^[12]. Following these discoveries, our team has been dedicated to the development of bioprocessing technologies aimed at removing hazardous compounds from ginkgo kernels, understanding the underlying mechanisms responsible for toxin removal, and promoting the practical application of probiotic fermentation technology in the ginkgo kernel processing industry (Supplementary Fig. S1). However, the exact reasons behind the removal or reduction of hazardous compounds in ginkgo kernels through probiotic fermentation remain unknown, which hinders the widespread use of this technology in real-world applications. Currently, two main speculations exist regarding this phenomenon: biodegradation and bio-adsorption. Although numerous studies have reported the microbial degradation of various toxins in environmental contexts^[13,14], there is a lack of research on the microbial degradation of ginkgo-related toxins and the corresponding metabolic pathways in the literature. Previous studies have shown that lactic acid bacteria, especially their cell wall

Detoxification of ginkgo kernel juice

components, can adsorb certain natural contaminants in foods and feeds^[15,16]. Given this, bio-degradation and bio-adsorption are two potential avenues to investigate and understand the mechanism behind reducing toxic components during the probiotic fermentation of ginkgo kernel juice.

Apart from probiotic fermentation, using macroporous resin for adsorption is another environmentally friendly option to reduce toxins in ginkgo kernel juice. Studies conducted by Zhang et al.^[17] and Kou & Wang^[18] have demonstrated that macroporous resin are effective in adsorbing 4'-O-methylpyridoxine and ginkgolic acids significantly, thereby enhancing the safety of ginkgo kernels. Consequently, it is reasonable to expect a synergistic effect when macroporous resin are added to ginkgo kernel juice during probiotic fermentation, leading to the removal of toxic constituents. From a microbiological standpoint, the microbial metabolism is likely to differ when adsorptive resin are present in ginkgo kernel juice, as they remove anti-nutritional and anti-microbial constituents, such as phenolics, from the broth^[19]. To our knowledge, the idea of simultaneously using probiotic fermentation and macroporous resin in ginkgo kernel juice has not yet been explored in the existing literature.

Following the above discussion, this study was conducted in three distinct parts. Firstly, the fermentative properties of autochthonous lactic acid bacteria isolated from ginkgo fruits were examined in ginkgo kernel juice with the addition of macroporous resin. The aim was to investigate how the resin impacted the removal of toxic constituents during the probiotic fermentation of ginkgo kernel juice. Secondly, the study focused on understanding the contributions of bio-degradation and bio-adsorption to the microbial removal of toxic ginkgolic acids. After thorough exploration, it was confirmed that bio-adsorption played a primary role in this process. In the third part, the mechanisms of ginkgolic acid adsorption by microbial strains and the combination of macroporous resin were investigated using experimental analysis and mathematical simulation (Fig. 1). The results of this study provide important insights into the microbial processes involved in the reduction of toxic components in ginkgo kernels and offer potential strategies to enhance the safety of products derived from ginkgo kernels.

Materials and methods

Materials

In this study, *Ginkgo biloba* kernels of the cultivar Dafozhi were provided by Taizhou Xiyang Food Co., Ltd. (China) Autochthonous lactic acid bacteria were isolated from ripe *Ginkgo biloba* fruits and characterised (Supplementary Table S1 & Supplementary Fig. S2). The isolated lactic acid bacteria were found to be strains of *Lactobacillus plantarum* and *Lactobacillus pentosus*. Moreover, four previously isolated microbial strains, namely *Lactobacillus plantarum* LSJ-TY-HYB-T7 (*L. plantarum* T7), *Lactobacillus plantarum* LSJ-TY-HYB-T9 (*L. plantarum* T9), *Lactobacillus fermentum* LSJ-TY-HYB-C22 (*L. fermentum* C22) and *Lactobacillus fermentum* LSJ-TY-HYB-L16 (*L. fermentum* L16) from different berry fruits, were also utilised in this study^[20]. To compare their abilities in removing toxins and enriching bioactives in ginkgo kernel juice after 48 h of fermentation, the selected microbial strains underwent evaluation (Supplementary Fig. S3). Based on the results, *Lactobacillus plantarum* TY-HYB-SYY-Y2 (*L. plantarum* Y2), *Lactobacillus plantarum* TY-HYB-SYY-Y4 (*L. plantarum* Y4), *Lactobacillus pentosus* TY-HYB-SYY-Y3 (*L. pentosus* Y3), and *Lactobacillus plantarum* LSJ-TY-HYB-T7 (*L. plantarum* T7) were chosen for further investigations. All these LAB strains were stored in 50% glycerol tubes and kept at -20°C for future use.

Experimental

Pretreatment with macroporous resin

The macroporous resin D101 and DA201 were pretreated following the method described by Wu et al.^[21]. The pretreatment process involves the following steps. The macroporous resin were soaked in 500 mL of 95% aqueous ethanol for 24 h. After soaking, the resin were thoroughly washed with deionised water. Then, 500 mL of 4% HCl was added to the resin for rinsing, which continued for 4 h. The resin were then washed with deionised water until their pH reached 7.0. Subsequently, 500 mL of 5% NaOH was used to rinse the resin for another 4 h. After the alkaline rinsing, the resin were washed with deionised water until their pH returned to 7.0. Finally, the pretreated resin were dried at 30°C until they reached a constant weight.

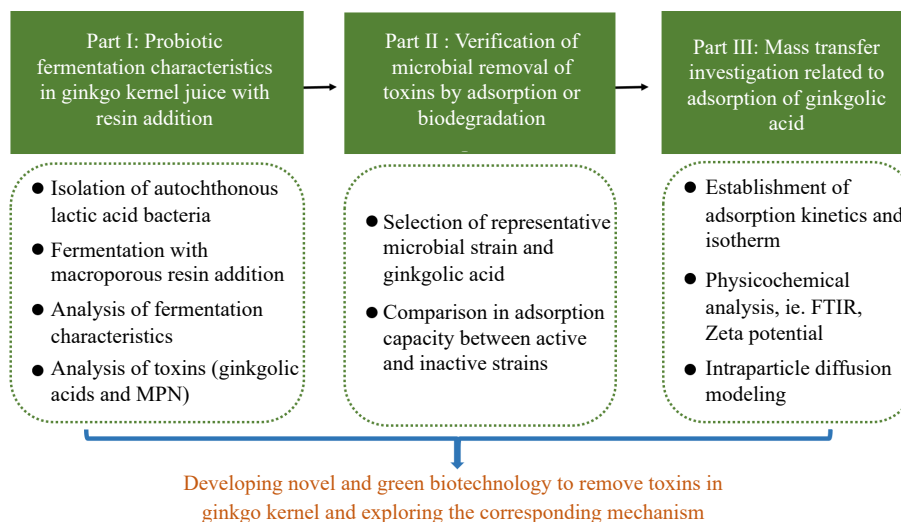


Fig. 1 Outline of this work illustrating investigations on the impact of probiotic fermentation combined with macroporous resin on eliminating toxic components in ginkgo kernel juice and exploring the underlying mechanism of toxin removal.

Preparation of ginkgo kernel juice

The method outlined by Wang et al. was followed to prepare ginkgo kernel juice^[12]. Fifty g of fresh *ginkgo biloba* kernels were taken and thoroughly washed. The washed kernels were ground in 250 mL of distilled water using a fruit juicer (MJ-BL25B22, Midea Holding Co., Ltd, China). For starch hydrolysis, 0.25 g of α -amylase (with an activity of 4,000 U/g) and 0.015 g of glucoamylase (with an activity of 100,000 U/g) were added to the ginkgo kernel juice. The mixture underwent enzymolysis at 60 °C for 2 h. After enzymolysis, the mixture was centrifuged at 5,000 rpm for 20 min to remove any insoluble precipitates. The ginkgo kernel juice was pasteurised at 90 °C for 20 min in a water bath (HH-5, Changzhou Wandasheng Experimental Instrument Co., Ltd, Changzhou, China) to ensure its safety and preservation. To facilitate the measurements of ginkgolic acids using the HPLC method, standard ginkgolic acid C15:1 and ginkgolic acid C13:0 were added to the pasteurised ginkgo kernel juice, making their contents 2.70 and 2.20 mg/L, respectively.

Fermentation of ginkgo kernel juice

Before fermentation, the pre-stored *Lactobacillus* strains were activated in 50 mL of MRS broth and then incubated at 30°C for 24 h in thermostatic incubator (PYX-DHS, Shanghai Yuejin Medical Equipment Co., Ltd, Shanghai, China). At the same time, the activated resin were sterilised at 121 °C for 20 min.

The sterilised ginkgo kernel juices were divided into two groups for the fermentation experiment. Activated *Lactobacillus* inoculum, 2.0% (v/v), was added directly to the juice in one group. In the other group, 5 g of sterilised resin were first added to the 250 mL juice samples, and then the 2.0% (v/v) inoculum was added. The initial cell counts in all the ginkgo kernel juice samples were approximately 7.34 ± 0.05 Log CFU/mL. Subsequently, the inoculated samples were cultured in a thermostatic oscillation incubator (SPH-100B Shipping Test Equipment Co., Ltd, China) at 30 °C and 200 rpm for 48 h. Samples were collected at different fermentation periods (0, 24, 48 h) for further analysis.

Comparative experiments investigating the variations in ginkgolic acid content in broths containing active and inactive *Lactobacillus* strains

The pre-stored *Lactobacillus plantarum* Y2 strains were activated in 50 mL of MRS broth and incubated at 30 °C for 16 h, allowing the strains to reach the stationary phase. After activation, the broth samples were divided into two groups. In one group, the samples were sterilised at 121 °C for 20 min, while the microbial strains remained alive in the other group. Then, 2 mg of standard ginkgolic acid C15:1 was added to 25 mL of the aforementioned MRS broth in both groups. The samples were further incubated at 30 °C and 200 rpm for 8 h in an orbital shaker to test the influence of both active and inactivated strains on the retention of ginkgolic acid.

After the incubation, the microbial strains were separated from the broths by centrifugation at 10,000 rpm for 10 min. The collected strains were mixed with methanol at 30 °C and 200 rpm for 1 h to investigate whether ginkgolic acid was desorbed from the microbial strains.

Adsorption studies

L. plantarum Y2 and macroporous resin D101 were chosen as the representative adsorbents for the investigation of the bio-adsorption mechanism.

Adsorption kinetics of ginkgolic acid

L. plantarum Y2 was first cultivated until it reached the stationary phase, and then it was inactivated following the procedure described above. The resulting microbial debris was collected by centrifugation and washed three times with deionised water. Subsequently, the microbial debris was dried at 30 °C to reach a constant weight and then milled into powders (Supplementary Fig. S4).

A standard aqueous solution of ginkgolic acid C15:1 at 10 mg/L was prepared. Separate mixtures of 100 mg microbial debris powders, 12.5 mg resin, and a combination of 100 mg microbial debris powders with 12.5 mg resin were added to 25 mL of the ginkgolic acid C15:1 solutions. The adsorption processes were carried out in a thermostatic oscillation incubator at 30 °C and 200 rpm. The concentration of ginkgolic acid C15:1 was measured at regular intervals until the adsorption equilibrium was achieved. The absorption capacity of each adsorbent is expressed in the following Eq (1):

$$q_{s,e} = \frac{(C_0 - C_t)}{m} V \quad (1)$$

where, $q_{s,e}$ is mass of ginkgolic acid adsorbed by the adsorbent at equilibrium (i.e. microbial strains, macroporous resin, and their mixture) (mg/g); C_0 is ginkgolic acid concentration in the solution at 0 min (mg/L); C_t is ginkgolic acid concentration in the bulk solution at t min (mg/L); m is weight of adsorbent (i.e. microbial strains, macroporous resin, and their mixture) (g); V is the volume of bulk solution of ginkgolic acid (mL).

Adsorption isotherm of ginkgolic acid

Standard aqueous solutions of ginkgolic acid C15:1 were prepared at concentrations of 5, 10, 12, and 15 mg/L. The microbial debris, the resin, and mixtures were added for each solution, following the procedures described previously. All adsorption processes were allowed to reach equilibrium. Afterwards, the concentration of ginkgolic acid C15:1 at equilibrium (C_e) and the adsorption capacity (q_e) were determined. The obtained data were then fitted to the Langmuir isotherm Eq (2):

$$q_s = \frac{q_m b C_e}{1 + b C_e} \quad (2)$$

where, q_s is mass of ginkgolic acid adsorbed by the adsorbent (i.e. microbial strains, macroporous resin, and their mixture) (mg/g); q_m is the maximum adsorption capacity of the adsorbent (i.e. microbial strains, macroporous resin, and their mixture) predicted by the Langmuir model (mg/g); b is langmuir constant (L/mg); C_e is ginkgolic acid concentration in the solution at equilibrium (mg/L).

Physicochemical analysis during fermentation

pH

The pH of ginkgo kernel juice was measured using a digital pH meter (PHS-3C, Shanghai INESA Scientific Instrument Co., Ltd, Shanghai, China).

Measurement of viable cell count

The viable cell counts were determined using the standard plate counting method after performing serial dilutions^[22]. The number of viable bacteria is expressed as Log CFU/mL.

Quantification of organic acid content

The analysis of individual organic acid contents in the ginkgo kernel juice was conducted using an HPLC system (LC-2010A, Shimadzu Tokyo, Japan) with separation achieved on the Agilent TC-C18 column (4.6 mm × 25 mm, 5.0 μm). The specific

Detoxification of ginkgo kernel juice

chromatographic method employed in this study can be referred to in our previous work^[23]. The concentrations of different organic acids are expressed as mg of each standard/L.

Quantification of monosaccharide content

The analysis of different monosaccharide contents in the ginkgo kernel juice followed the methodology described in our previous work^[24]. Calibration curves were established using various monosaccharide standards. The concentrations of different monosaccharides are expressed as mg of each standard/L.

Quantification of ginkgolic acid content

In this study, the types of ginkgolic acids present in the ginkgo kernel juice were initially identified using HPLC-MS, leading to the tentative identification of three ginkgolic acids (Supplementary Text 1 & Supplementary Table S2). Subsequently, the contents of two representative ginkgolic acids, namely ginkgolic acid C15:1 and ginkgolic acid C13:0, were quantified in the ginkgo kernel juice using a Waters 1525 HPLC system (Mirford, USA) connected to a YMC Carotenoid column (4.6 mm × 150 mm, 3.0 μm). The chromatographic conditions were adopted from a previous study by Wang et al.^[12]. Specifically, the mobile phase consisted of 3% glacial acetic acid in deionised water:methanol (8:92, v/v), and the elution was carried out at a flow rate of 0.8 mL/min. The detection wavelength and column temperature were set at 310 nm and 30 °C, respectively. An injection volume of 20 μL was used for the analysis. The content of each ginkgolic acid in the ginkgo kernel juice is expressed as mg of each standard/L.

Quantification of 4'-O-methylpyridoxine (MPN) content

MPN in the ginkgo kernel juice was quantified using the same Shimadzu LC-2010A device coupled with an Agilent TC-C18 column (4.6 mm × 250 mm, 5.0 μm). The chromatographic conditions were adapted from a previous study by Zou et al.^[25]. The mobile phase A used was a 5.0 mmol/L potassium phosphate solution containing 5.0 mmol/L sodium pentane sulfonate (pH 2.5), while mobile phase B consisted of acetonitrile. The gradient program for elution was as follows: 0–10 min, 4%–8% B; 10–15 min, 8%–10% B; 15–20 min, 10%–8% B; 20–40 min, 8–4% B. The flow rate was set at 1 mL/min. The column temperature was maintained at 30 °C, and the detection wavelength was set at 292 nm. An injection volume of 20 μL was used for the analysis. The results are expressed as mg of each standard/L.

Quantification of total phenolics content

The total phenolics content in the ginkgo kernel juice was measured using the Folin-Ciocalteu method using a UV-Vis spectrophotometer (TU-1900, Persee General Instruments Co., Ltd, Shanghai, China), as described in detail in our previous study^[26]. Gallic acid was employed as the standard substance for calibration. The results are reported as mg of gallic acid equivalent /L.

Physicochemical analysis during adsorption

Porosity

The porosity (ϵ_p) of the adsorbent was estimated using the following Eq (3):^[27]

$$\epsilon_p = 1 - \frac{\rho_p}{\rho_s} \quad (3)$$

where, ρ_p is apparent density of adsorbent (i.e. microbial strains, macroporous resin, and their mixture) (g/mL); ρ_s is solid density of

adsorbent (i.e. microbial strains, macroporous resin, and their mixture) (g/mL).

In this study, the porosity values for the debris powders of *L. plantarum* Y2, macroporous resin D101, and their mixture were determined as follows: 0.005, 0.238 and 0.057, respectively. The low porosity indicates that microbial debris can be considered solid materials with limited pore space.

Particle size distribution

The particle size distribution of the adsorbents was determined using a laser particle size analyser (Mastersizer 2000, Malvin Instruments Co., Ltd, UK). The average particle sizes for microbial debris, resin, and their mixture were 30.92 μm, 127.10 μm, and 38.70 μm, respectively.

Zeta potential

The Zeta potentials of the dispersions before and after adsorption were determined using the Nano ZS90 Zetasizer (Malvin Instruments Co., Ltd, UK). The temperature was maintained at 25 °C. The dispersant and the number of tests were set to 'water' and 'Automatic' respectively. The measurements were performed in triplicate to ensure accuracy and reliability.

FT-IR

The microbial debris, resin, and their mixture before and after adsorption were collected and dried to remove any residual water. Subsequently, the dried materials were milled into powders. For the FT-IR analysis, 1 mg of each powder was mixed separately with 100 mg of KBr and then pressed into flakes with a height of 2 mm. The resulting flakes were scanned using the Nicolet IR200 FT-IR spectroscopy (Nicolet IR 200, Thermo Electron Corporation, Massachusetts, USA) in the range of 4000 to 400 cm⁻¹. This FT-IR analysis was performed to investigate any changes or interactions in the chemical compositions of the adsorbents before and after the adsorption process.

Mass transfer during adsorption

The pore volume and surface diffusion model (PVSDM) was employed to analyse the concentration decay of ginkgolic acid during physisorption. This model incorporates several phenomena, including external mass transfer of ginkgolic acid from the bulk solution to the adsorbent surface, intraparticle diffusion (surface or pore volume diffusion of ginkgolic acid inside the adsorbent particle), and instantaneous adsorption of ginkgolic acid on the active sites^[28–30]. To simplify the model, the following assumptions were considered^[31,32]:

(1) Microbial debris, resin, and their mixture were assumed to have spherical and isotropic geometry. As a result, the intraparticle diffusion mode of ginkgolic acid was considered to be one-dimensional radial diffusion.

(2) The PVSDM model depicting the adsorption of ginkgolic acid by various adsorbents, based on the assumptions of insignificant convective mass transfer inside the pores and constant pore volume diffusion coefficient (D_{ep}) and surface diffusion coefficient (D_s), is expressed as follows (Eq 4):

$$\epsilon_p \frac{\partial C_s}{\partial t} + \rho_p \frac{\partial q_s}{\partial t} = \frac{1}{r^2} \frac{\partial}{\partial r} \left(r^2 \left(D_{ep} \frac{\partial C_s}{\partial r} + D_s \rho_p \frac{\partial q_s}{\partial r} \right) \right) \quad (4)$$

where, ϵ_p is porosity of adsorbent (i.e. microbial strains, macroporous resin, and their mixture); C_s is ginkgolic acid concentration in the solution within the porous space of adsorbent (i.e. macroporous resin alone or the mixture of resin and microbial strains) (mg/L); t is adsorption time (min); D_{ep} is pore volume diffusion coefficient of ginkgolic acid (m²/s); D_s is surface diffusion coefficient of ginkgolic acid (m²/s).

The initial conditions are defined as follows (Eq 5):

$$t = 0 \quad C_s = 0 \quad q_s = 0 \quad 0 \leq r \leq R \quad (5)$$

where, R is radius of adsorbent (i.e. microbial strains, macroporous resin and their mixture) (cm)

The boundary conditions are described as follows (Eqs 6 & 7):

$$\left. \frac{\partial C_s}{\partial r} \right|_{r=0} = 0 \quad (6)$$

$$D_{ep} \left. \frac{\partial C_s}{\partial r} \right|_{r=R} + D_s \rho_p \left. \frac{\partial q_s}{\partial r} \right|_{r=R} = k_L (C_L - C_s) \quad (7)$$

where, k_L is external mass transfer coefficient of ginkgolic acid (m/s); C_L is total ginkgolic acid concentration in the solution (mg/L).

Since the adsorption on active sites occurred much faster than intraparticle diffusion, it was assumed that the local adsorption equilibrium on the solid-liquid interface could be achieved instantaneously^[33]. Consequently, the term C_s in the *PVSDM* model can be replaced by q_s using the Langmuir relationship (Eq 2). Subsequently, Eqs (4, 6, & 7) can be transformed into Eqs (8, 9, & 10), respectively as follows:

$$\left(\varepsilon_p \frac{q_m b}{(q_m b - b q_s)^2} + \rho_p \right) \frac{\partial q_s}{\partial t} = \frac{1}{r^2} \frac{\partial}{\partial r} \left(r^2 \left(D_{ep} \frac{q_m b}{(q_m b - b q_s)^2} + D_s \rho_p \right) \frac{\partial q_s}{\partial r} \right) \quad (8)$$

$$\left. \frac{q_m b}{(q_m b - b q_s)^2} \frac{\partial q_s}{\partial r} \right|_{r=R} = 0 \quad (9)$$

$$D_{ep} \left. \frac{q_m b}{(q_m b - b q_s)^2} \frac{\partial q_s}{\partial r} \right|_{r=R} + D_s \rho_p \left. \frac{\partial q_s}{\partial r} \right|_{r=0} = k_L (C_L - C_s) \quad (10)$$

To solve the *PVSDM* model, the two key parameters, D_{ep} and k_L , need to be calculated. D_{ep} is closely related to the features of the adsorbent, adsorption temperature, and adsorbate solvent^[34]. It can be estimated using the following Eq (11)^[31,35]:

$$D_{ep} = \frac{\varepsilon_p}{\tau} D_{AB} \quad (11)$$

where, D_{AB} is molecular diffusion coefficient of ginkgolic acid at infinite dilution (m²/s); τ is tortuosity factor of adsorbent (i.e. microbial strains, macroporous resin, and their mixture). The values of τ and D_{AB} are calculated using Eqs (12 & 13), respectively^[36,37].

$$\tau = \frac{(2 - \varepsilon_p)^{-1/3}}{\varepsilon_p} \quad (12)$$

$$D_{AB} = 7.4 \times 10^{-8} \frac{T(\varphi M_B)^{0.5}}{n_B V_A^{0.6}} \quad (13)$$

where, T is adsorption temperature (°C or K); φ is association factor of water; V_A is molecular volume of ginkgolic acid (cm³/mol); M_B is molecular weight of water (mol/g); n_B is the viscosity of water at 30 °C (cp).

The required and calculated values of the indicated parameters are listed in [Supplementary Table S3](#).

The external mass transfer coefficient (k_L) can be obtained based on the concentration decay curve of ginkgolic acid in the solution during the first two sampling periods^[38,39]. It is calculated using the following Eq (14):

$$\left(\frac{d \left(\frac{C_L}{C_0} \right)}{dt} \right)_{t \rightarrow 0} = - \frac{m S k_L}{V} \quad (14)$$

$$S = \frac{3}{R \rho_p} \quad (15)$$

where, S is the surface area of adsorbent (i.e. microbial strains, macroporous resin, and their mixture) (cm²/g).

The *PVSDM* model was solved using the *pdepe* function in Matlab R2009a (The MathWorks, Inc., MA, USA). To obtain the surface diffusion coefficient (D_s), it was initially assigned a value and then iteratively adjusted to minimise the differences between the experimental ($q_{i,e}$) and predicted values ($q_{i,p}$) of ginkgolic acid adsorption. During this optimisation process, the *AAD* (Eq 16) and R^2 (Eq 17) values were calculated to assess the model's predictive accuracy.

$$AAD\% = \left(\frac{\sum_{i=1}^n (|q_{i,e} - q_{i,p}| / q_{i,e})}{n} \right) \times 100 \quad (16)$$

$$R^2 = 1 - \frac{\sum_{i=1}^n (q_{i,e} - q_{i,p})^2}{\sum_{i=1}^n (q_{e,mean} - q_{i,p})^2} \quad (17)$$

where, *AAD* is absolute average deviation (%); $q_{i,e}$ is the experimentally measured mass of ginkgolic acid adsorbed by the adsorbent (i.e. microbial strains, macroporous resin, and their mixture) (mg/g); $q_{i,p}$ is the predicted mass of ginkgolic acid adsorbed by the adsorbent (i.e. microbial strains, macroporous resin, and their mixture) (mg/g); n is the number of experimental data; R^2 is coefficient of determination; $q_{e,mean}$ is the mean value of adsorption capacity for adsorbent (i.e. microbial strains, macroporous resin, and their mixture) (mg/g).

Based on the numerical results, the mass flux due to the pore volume diffusion (N_{AP}) and surface diffusion (N_{AS}) inside the adsorbent were estimated using Eqs (18 & 19), respectively^[40]:

$$N_{AP} = -D_{ep} \frac{\partial C_s}{\partial r} \quad (18)$$

$$N_{AS} = -D_s \rho_p \frac{\partial q_s}{\partial r} \quad (19)$$

Finally, the percentage of surface diffusion contribution (*SDCP%*) is determined using the following Eq (20)^[34]:

$$SDCP\% = \frac{\|N_{AS}\|}{\|N_{AS}\| + \|N_{AP}\|} \times 100 \quad (20)$$

Statistical analysis

All experimental data were collected in triplicate and expressed as mean \pm standard deviation. A one-way variance analysis (ANOVA) was performed using SPSS Statistics 20.0 (IBM Corp., NY, USA) to compare the mean values. Statistical significance was considered at the $p < 0.05$ probability level. Principal component analysis (PCA) was conducted using Origin 2022 (Origin, Inc., USA) for multivariate analysis. Mass transfer investigations were conducted using Matlab R2009 (The MathWorks, Inc., MA, USA).

Results and discussion

Fermentation of ginkgo kernel juice using lactic acid bacteria with the incorporation of macroporous resin

pH and viable cell counts

Figure 2 illustrates the changes in pH value and viable cell counts during the probiotic fermentation of ginkgo kernel juice. As shown in Fig. 2a, the initial pH value of the ginkgo kernel juice was 4.78 ± 0.02 . After 48 h of fermentation, the pH values in all samples decreased to a range of 3.13–3.49. Notably, the sample fermented by *L. plantarum* T7 exhibited a

Detoxification of ginkgo kernel juice

higher pH value than the other samples. This observation could be attributed to the fact that *L. plantarum* T7 was isolated from cherry tomato, whereas the other microbial strains were autochthonous lactic acid bacteria isolated from ginkgo fruit. Generally, autochthonous microorganisms are more adaptable to the ginkgo kernel environment and can utilise the nutrients in the ginkgo kernel, leading to increased lactic acid synthesis^[41]. Figure 2b shows that after 24 h of fermentation, the viable cell counts in the ginkgo kernel juices increased to a range of 8.45–8.97 Log CFU/mL, depending on the specific microbial strains utilised. Subsequently, the viable cell counts did not exhibit significant changes throughout the fermentation process. On the other hand, adding macroporous resin at the beginning of fermentation did not have any noticeable impact on the decline of pH value and microbial growth.

Organic acid profile

The PCA analysis of the organic acid profile during probiotic fermentation with the simultaneous addition of macroporous resin is illustrated in Fig. 3a & b, with the contents of nine individual organic acids in ginkgo kernel juices presented in Supplementary Table S4. The first two principal components (PCs) accounted for 77.5% of the total variance associated with

the organic acid data, indicating that these two PCs effectively captured the changes in the organic acid profile during fermentation. As depicted in Fig. 3a, the unfermented samples, with and without the addition of macroporous resin, were observed to be located close to each other, suggesting that the presence of macroporous resin did not lead to significant adsorption of organic acids in the ginkgo kernel juice. This result aligns with our previous study on the adsorption of crude anthocyanin extracts using macroporous resin^[27]. On the other hand, a clear separation between the fermented and unfermented samples was evident based on their organic acid profiles.

In Fig. 3b, the PC1 values of ginkgo kernel juice fermented by all microbial strains showed an increasing trend with fermentation time. By analysing the score and loading plots, it could be observed that fumaric acid, malic acid, and citric acid exhibited negative PC1 values, indicating their decline during fermentation. On the other hand, oxalic acid, lactic acid, shikimic acid, and succinic acid had positive PC1 values, indicating their increase during fermentation. The specific data further confirmed the changes in organic acid contents during fermentation. For example, the malic acid content in unfermented ginkgo kernel juice was measured as 199.86 ± 21.11 mg/L. After

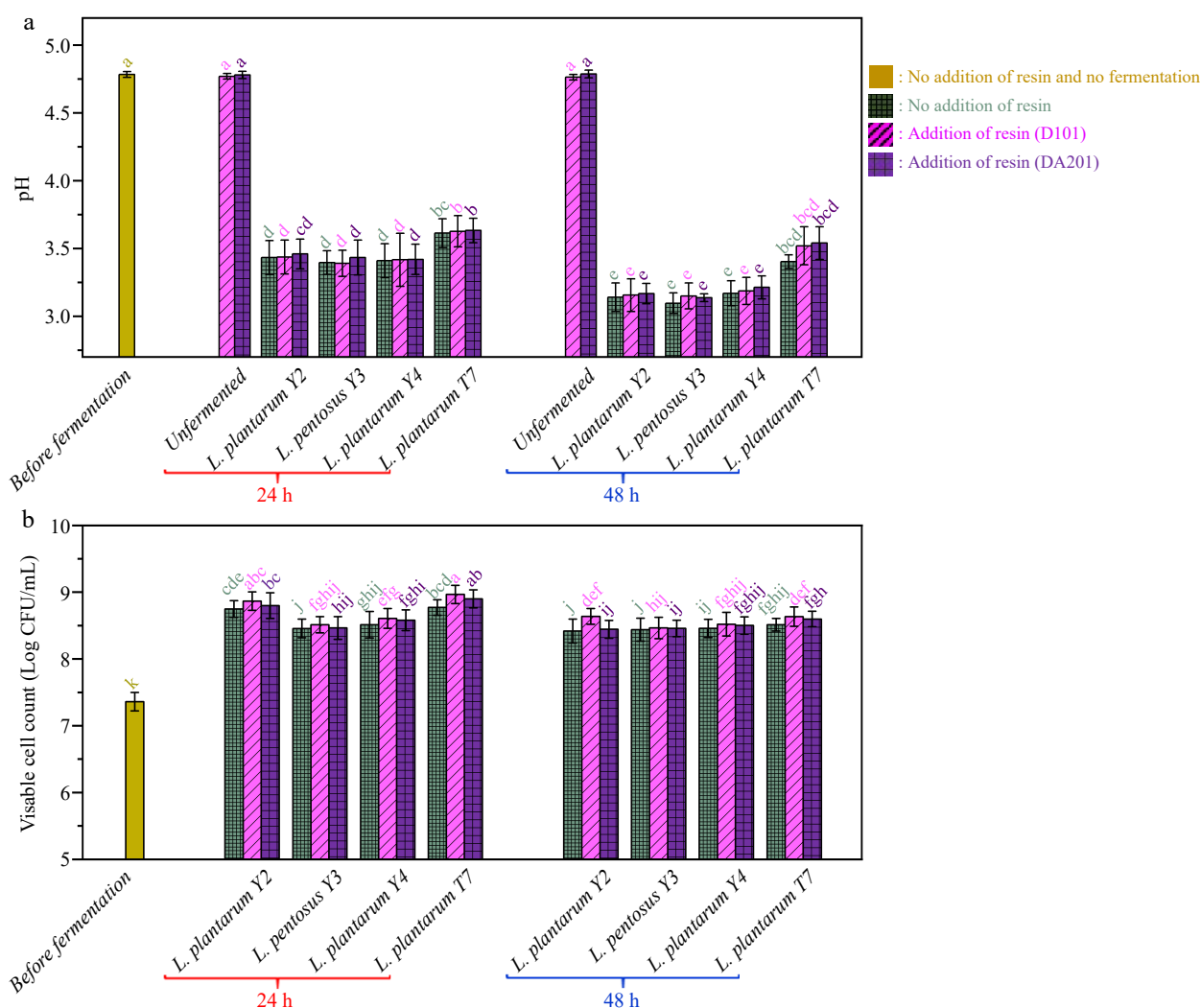


Fig. 2 (a) pH variations and (b) viable cell count changes during probiotic fermentation of ginkgo kernel juices with and without the addition of macroporous resin.

48 h of fermentation without the addition of macroporous resin, the malic acid content in the samples fermented by *L. plantarum* Y2, *L. pentosus* Y3, *L. plantarum* Y4, and *L. plantarum* T7 decreased by approximately 70.17%, 79.67%, 79.73%, and 40.27%, respectively. Moreover, the lactic acid production in the samples fermented by *L. plantarum* Y2, *L. pentosus* Y3, *L. plantarum* Y4, and *L. plantarum* T7 reached 779.69 ± 15.40 mg/L, 796.60 ± 6.26 mg/L, 1077.70 ± 34.92 mg/L, and 689.62 ± 44.94 mg/L, respectively. Similar results were obtained in our previous studies on probiotic fermentation of blueberry juice and apple juice, where PCA based on organic acid profiles effectively discriminated fermented samples at different stages of fermentation^[12,20,23,42].

Furthermore, the scatter plot of the fermented samples with and without adding macroporous resin at the same fermentation period showed their proximity, indicating that any differences in organic acid profiles among these samples could be considered negligible. This observation provides additional evidence to support the notion that macroporous resin had minimal impact on the microbial metabolism of organic acids during fermentation. Despite the theoretical capacity of resin to adsorb certain juice components, such as phenolics and terpene lactone, the microbial processes responsible for organic acid metabolism seemed to proceed undisturbed by the presence of resin^[43,44].

Monosaccharides

The contents of six monosaccharides in ginkgo kernel juice during probiotic fermentation are presented in [Supplementary Table S5](#). These monosaccharides primarily originated from the enzymolysis with α -amylase and glycolytic enzyme during the preparation of ginkgo kernel juice. The PCA analysis of monosaccharide data is depicted in [Fig. 3c & d](#). The first two PCs accounted for 94.0% of the total variance in monosaccharides, indicating that these two PCs adequately captured the changes in monosaccharide profiles during fermentation. Similar to [Fig. 3a](#), [Fig. 3c](#) shows that the unfermented samples with and without adding macroporous resin are closely clustered. This observation reaffirms that macroporous resin did not interfere with the availability of these carbon sources required for microbial growth. Moreover, PC1 was instrumental in distinguishing the samples at different fermentation periods, with the PC1 value of fermented ginkgo kernel juices decreasing over time. In conjunction with [Fig. 3d](#), it is evident that all the analysed monosaccharides exhibited positive PC1 values, indicating a continuous decline in the contents of rhamnose, glucose, galactose, xylose, fructose, and arabinose during fermentation. During lactic acid fermentation, glucose was identified as the primary carbon source. After 48 h of fermentation without the addition of macroporous resin, the glucose contents in various samples were reduced from 20.58 ± 3.64

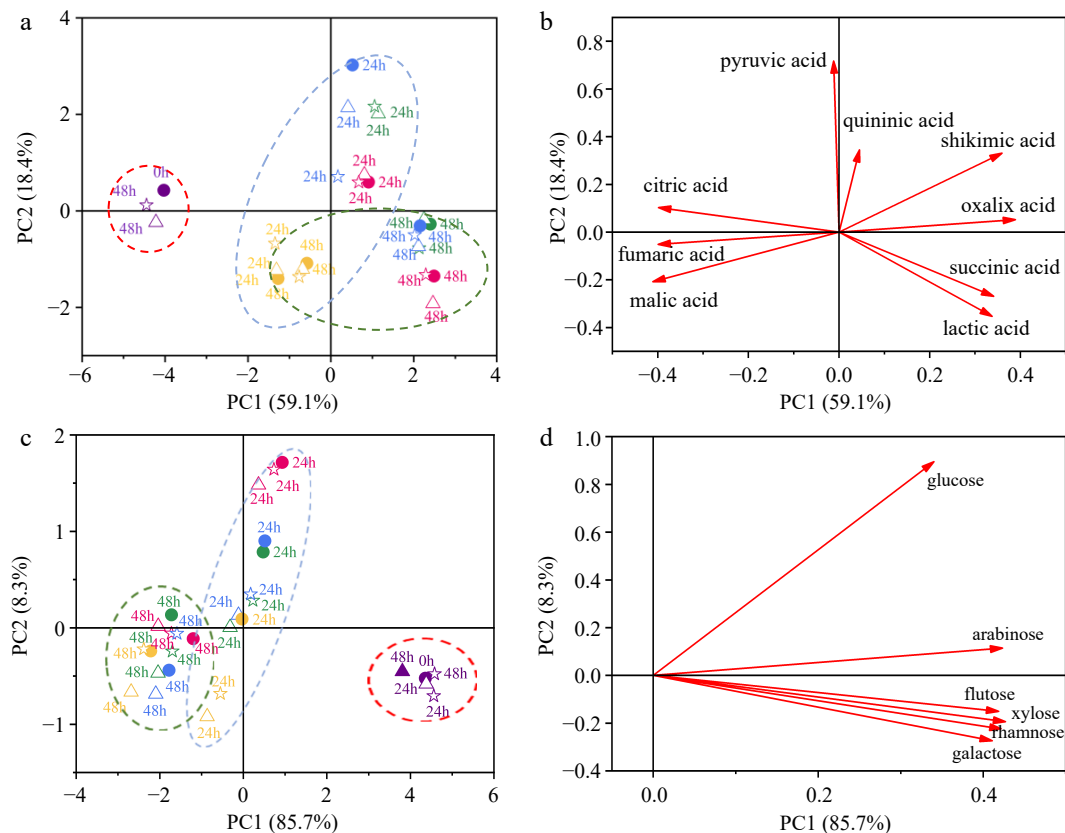


Fig. 3 Principal component analysis (PCA) conducted on the organic acid profile and monosaccharide profile during probiotic fermentation of ginkgo kernel juice, with and without the addition of macroporous resin. (a) Score plot based on the organic acid profile. (b) Loading plot based on the organic acid profile. (c) Score plot based on the monosaccharide profile. (d) Loading plot based on the monosaccharide profile. (●) Fermentation of samples without the addition of macroporous resin; (△) Fermentation of samples with the addition of macroporous resin D101; (☆) Fermentation of samples with the addition of macroporous resin DA201. Purple: unfermented samples; Red: fermentation of samples by *L. plantarum* Y2; Green: fermentation of samples by *L. pentosus* Y3; Blue: fermentation of samples by *L. plantarum* Y4; Yellow: fermentation of samples by *L. plantarum* T7.

Detoxification of ginkgo kernel juice

mg/L to (3.20 ± 0.30) – (9.37 ± 0.91) mg/L, which varied depending on the specific lactic acid bacteria utilised. A previous study by Wang et al.^[12] reported that three commercial lactic acid bacteria consumed more than 80% of glucose during the probiotic fermentation of ginkgo kernel juice.

Furthermore, the fermented samples with and without the addition of macroporous resin are distributed together, suggesting that macroporous resin did not impact the microbial metabolism of monosaccharides, especially the utilisation of carbon sources by the microorganisms.

Ginkgolic acids

Fig. 4a & b show the changes in the contents of two toxic ginkgolic acids, ginkgolic acid C15:1 and ginkgolic acid C13:0, during fermentation. In the unfermented ginkgo kernel juice, the initial contents of ginkgolic acids C15:1 and C13:0 were measured as 2.71 ± 0.19 mg/L and 2.20 ± 0.22 mg/L, respectively. Notably, both macroporous resin, D101 and DA201, demonstrated the ability to adsorb ginkgolic acids, as evidenced by their contents in the unfermented ginkgo kernel juice decreasing by 36.46% and 27.38%, respectively, after 48 h of immersion. The reduction in ginkgolic acid levels due to the adsorption by macroporous resin is significant. It could be crucial for improving the safety of ginkgo kernel products, as ginkgolic acids are known to be major toxic constituents associated with various health risks, including cytotoxicity, hepatotoxicity, embryotoxicity, neurotoxicity, allergies, and inhibition of human enzyme systems^[45,46].

During the probiotic fermentation process using the applied microbial strains, the ginkgolic acid contents in the juices decreased. After 48 h of fermentation without the use of macroporous resin, the contents of ginkgolic acids C15:1 and C13:0 were reduced to 1.67 ± 0.21 mg/L by *L. plantarum* Y2, 1.99 ± 0.25 mg/L by *L. pentosus* Y3, 1.99 ± 0.37 mg/L by *L. plantarum* Y4, and 2.17 ± 0.25 mg/L by *L. plantarum* T7, respectively. It is widely accepted in various studies on ginkgolic acids toxicity that food products containing ginkgolic acid content lower than 5 ppm (approximately 5 mg/L) are considered safe^[47–49]. Therefore, the current study confirms that fermentation using the selected lactic bacteria effectively removes the toxic ginkgolic acids, making the juices safe for consumption.

On the contrary, the probiotic fermentation exhibited a synergistic effect when combined with adsorption using macroporous resin to remove ginkgolic acids. Compared to fermentation alone, adding macroporous resin resulted in a greater reduction of ginkgolic acids, with macroporous resin D101 showing more effectiveness in decreasing ginkgolic acid C13:0 and C15:1 than resin DA201. Specifically, after 48 h of fermentation with the addition of macroporous resin D101, the ginkgolic acid C13:0 content in all samples dropped below 0.05 mg/L. In contrast, in the samples without adding macroporous resin D101, the ginkgolic acid C13:0 content remained above 0.87 mg/L. Overall, the combined probiotic fermentation with macroporous resin adsorption reduced more than 69.1% of ginkgolic acid C13:0 and 69.7% of ginkgolic acid C15:1 in the ginkgo kernel juice. In the studies conducted by Fan et al.^[9] and Dong et al.^[50], different methods were explored to reduce the content of ginkgolic acids in processed samples of ginkgo kernels. Specifically, steaming, microwave irradiation, and liquid-liquid microextraction were applied, leading to reductions of 54.5%, 27.0%, and 74.4%, respectively, in the ginkgolic acid levels. However, the probiotic fermentation process and

adding macroporous resin prove to be a competitive and effective method for lowering toxic ginkgolic acids in ginkgo kernel-related products.

4'-O-methylpyridoxine (MPN)

MPN is present in various parts of the ginkgo tree, including the leaves and fruit. It is an analog of vitamin B6 and has been associated with adverse health effects, such as vomiting, tonic-clonic convulsions, and neurotoxic consequences, due to its ability to reduce the synthesis of γ -aminobutyric acid^[45]. Fig. 4c illustrates the initial MPN content in ginkgo kernel juice before fermentation, measured at 23.48 ± 1.40 mg/L. Similar to the behavior of ginkgolic acids, MPN was also subjected to adsorption by the macroporous resin used in this study. Following adsorption without fermentation for 48 h, the MPN content in the ginkgo kernel juices, with resin DA201 and D101 additions, decreased to 18.93 ± 0.74 mg/L and 17.90 ± 0.25 mg/L, respectively.

The lactic acid fermentations conducted without adding macroporous resin resulted in a noticeable reduction in MPN content in the ginkgo kernel juices. After 48 h of fermentation without using macroporous resin, the MPN contents decreased by 61.1% to 65.6%, depending on the specific microbial strains employed in the fermentation process. Interestingly, during the initial 24 h of fermentation, the probiotic fermentation exhibited a synergistic effect when combined with macroporous resin adsorption in removing MPN. For example, in samples fermented by *L. plantarum* Y2, the MPN content was measured at 10.21 ± 1.03 mg/L with the addition of macroporous resin DA201, while it was 13.69 ± 1.49 mg/L without the resin. However, after 48 h of fermentation, there was no significant difference in MPN content between the fermentations conducted in the presence and absence of macroporous resin. The studies conducted by Hong et al.^[51] and Zou et al.^[52] investigated different methods to reduce MPN content in ginkgo kernel juices. Steaming and fermentation by *Eurotium cristatum* decreased MPN content by 28.6% and 40.2%, respectively, in the processed juices. Comparatively, the current lactic acid fermentation process, with the addition of macroporous resin, proves to be a promising and more effective method for reducing toxic MPN in ginkgo kernel juice.

Total phenolics

Phenolics are essential bioactive compounds in ginkgo kernels, especially from the flavonoid family. As shown in Fig. 4d, the initial phenolic content of ginkgo kernel juice was measured at 158.69 ± 3.85 mg/L. Following a 48 h adsorption process using macroporous resin D101 and DA201, the phenolic content decreased to 132.24 ± 5.80 and 126.93 ± 4.02 mg/L, respectively.

In the fermentation groups without adding macroporous resin, the total phenolic contents in the ginkgo kernel juices increased to a range of 178.87 to 184.36 mg/L after 48 h of fermentation. There was no significant difference in total phenolic contents among these samples. During probiotic fermentation, the phenolic compounds underwent complex bioconversions facilitated by extracellular enzymes, such as phenolic acid decarboxylase and phenolic acid reductase, as previously reported^[42,53]. These enzymatic actions resulted in changes to the total phenolic contents in the ginkgo kernel juices during the fermentation process. As anticipated, the total phenolic contents in the fermented samples with the addition

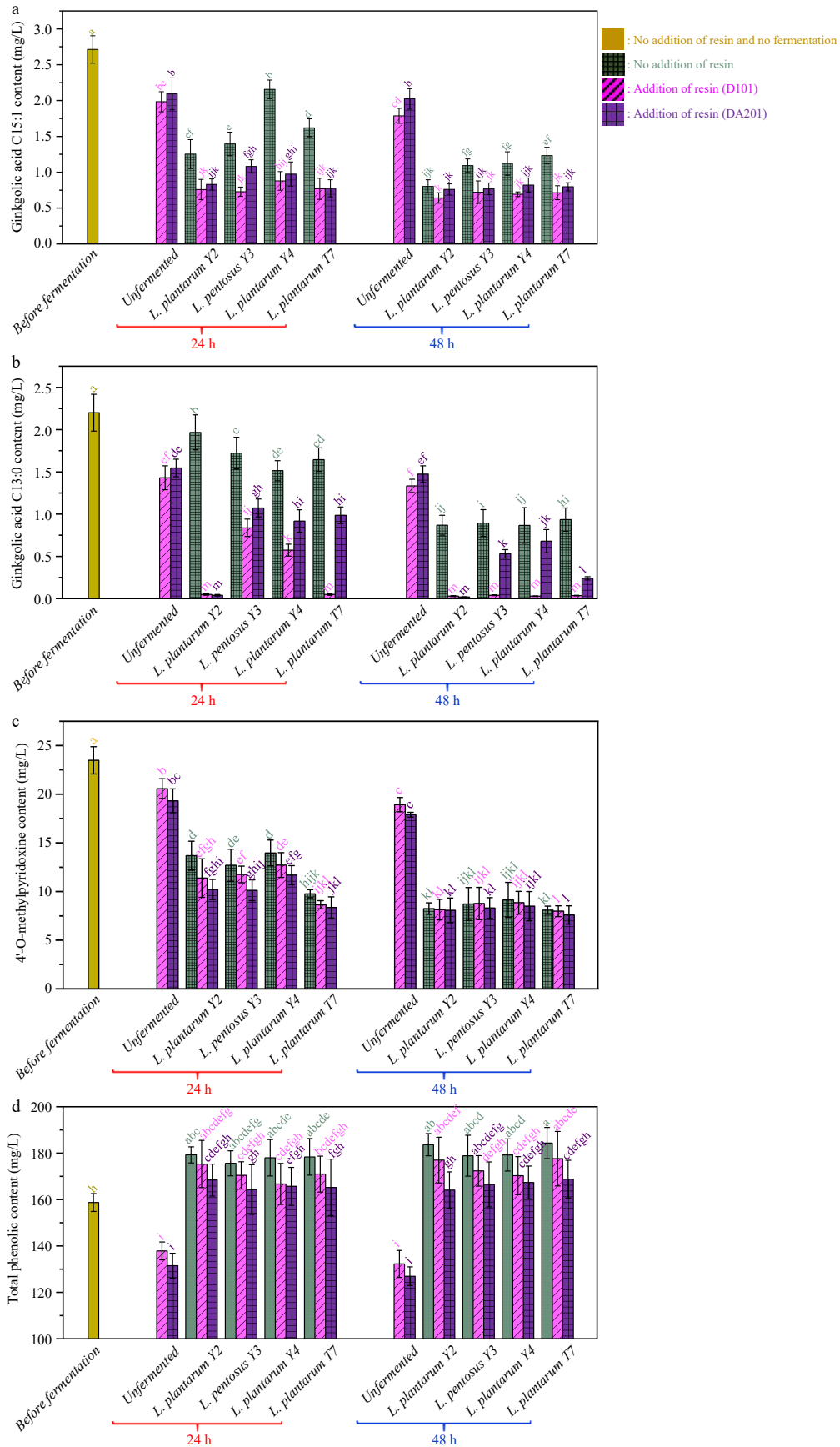


Fig. 4 Changes in the contents of (a) ginkgolic acid C15:1, (b) ginkgolic acid C13:0, (c) 4'-O-methylpyridoxine and (d) total phenolics during probiotic fermentation of ginkgo kernel juices with and without the addition of macroporous resin.

Detoxification of ginkgo kernel juice

of macroporous resin were lower than in the counterparts without resin, mainly due to the physisorption of phenolic compounds by the resin. However, even after 48 h of fermentation, the total phenolic contents in all the samples remained higher than in the samples before fermentation.

Review of the influence of macroporous resin adsorption on probiotic fermentation of ginkgo kernel juice

Based on the above results, it is evident that the physisorption of various components present in ginkgo kernel juice, such as ginkgolic acids, MPN, and phenolics, by macroporous resin, did not have a noticeable impact on the fermentation characteristics of *Lactobacillus* species. Adding macroporous resin during fermentation did not result in significant differences in pH, viable cell numbers, organic acid profile, and monosaccharide profile compared to fermentations conducted without resin addition. As a result, it can be tentatively concluded that the adsorption by resin did not interfere with the essential metabolic pathways of the microorganisms, such as glycolysis for glucose consumption and pyruvic acid formation, the tricarboxylic acid cycle involving succinic acid, citric acid, malic acid, as well as anaerobic glycolysis. Indeed, both ginkgolic acids and phenolic compounds have been reported to possess antibacterial activities against lactic acid bacteria^[54]. Given this information, it is reasonable to speculate that these growth inhibitors in the broth can potentially impact microbial metabolism during the fermentation process. Therefore, it is important to conduct a thorough and in-depth investigation to fully understand the roles of interference factors on probiotic fermentation.

Comparison of the variations in ginkgolic acid content in the broths containing active and inactive *Lactobacillus* strains

The first part of the study has demonstrated that probiotic fermentation, both with and without macroporous resin adsorption, effectively reduces toxic components in ginkgo kernel juices. However, the reasons behind these reductions have not been fully explored and remain unknown. To delve deeper into understanding the mechanisms and interactions involved, *L. plantarum* Y2 and ginkgolic acid C15:1 were chosen as representative microbial strains and toxic constituents for the next parts of the investigations, respectively.

To investigate whether the decline of ginkgolic acids in the ginkgo kernel juice is primarily due to microbial degradation,

microbial adsorption, or a combination of both, a comparison was made between the changes in ginkgolic acid C15:1 content in broths containing active and inactive *L. plantarum* Y2. In Fig. 5a, it is shown that after incubation for 8 h, the ginkgolic acid C15:1 content in both MRS broths containing active and inactive *L. plantarum* Y2 decreased from 80 mg/L to approximately 40 mg/L. Importantly, the two samples had no significant difference ($p > 0.05$) in the ginkgolic acid C15:1 content. This indicates that the ability of active *L. plantarum* Y2 to remove ginkgolic acid C15:1 was equivalent to that of the inactive strains. Then, the microbial strains (both active and inactive) were collected and washed with methanol to elute any ginkgolic acid C15:1 that may have been adsorbed by the cells. In Fig. 5b, it is shown that the amounts of ginkgolic acid C15:1 eluted from the inactive and active strains were measured as 0.63 ± 0.06 mg and 0.69 ± 0.07 mg, respectively.

Indeed, the comparison between active and inactive *L. plantarum* Y2 strains and the subsequent analysis of ginkgolic acid C15:1 content in the broths and eluted from the strains strongly support the conclusion that bio-adsorption plays a significant role in the reduction of toxic ginkgolic acid during the lactic acid fermentation of ginkgo kernel juices.

Adsorption of ginkgolic acid by *L. plantarum*, macroporous resin, and their mixture

The above part of the study demonstrated that the reduction of ginkgolic acid C15:1 during the lactic acid fermentation of ginkgo kernel juices was partially attributed to bacterial adsorption. The mass transfer mechanisms of ginkgolic acid C15:1 adsorption by three key components were studied further to investigate the underlying mechanisms of this adsorption process: *L. plantarum* Y2, resin D101, and their mixture.

Adsorption kinetic analysis

Fig. 6a presents the adsorption kinetic curves of microbial strains powders, macroporous resin, and their mixture at 30 °C. The data reveal clear differences in the adsorption abilities of these different adsorbents. The adsorption process for microbial strains powders took approximately 360 min to reach equilibrium, with an equilibrium adsorption capacity of 1.98 ± 0.29 mg/g. In contrast, macroporous resin demonstrated much faster adsorption kinetics, reaching equilibrium within about 20 min and exhibiting a higher adsorption capacity of 15.73 ± 1.01 mg/g. This significant difference can be attributed to the

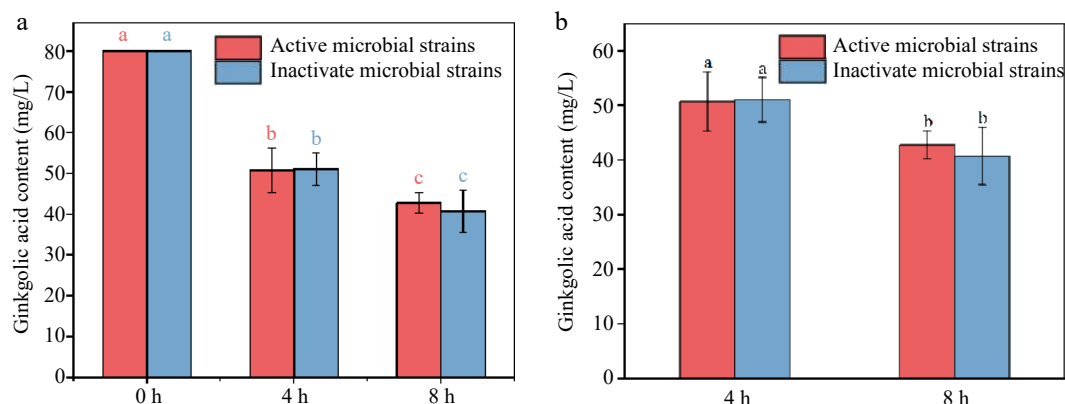


Fig. 5 (a) Changes in ginkgolic acid C15:1 content in the broths containing active and inactive *L. plantarum* Y2 and (b) amount of ginkgolic acid C15:1 desorbed from the microbial strains with previous adsorption.

porous structure and large specific surface area of the macroporous resin, which allows it to bind more ginkgolic acid efficiently^[55]. Moreover, the microbial strains and macroporous resin displayed faster adsorption kinetics, reaching equilibrium within 20 min, similar to the pure resin. Additionally, the equilibrium adsorption capacity for the mixture was measured at 2.18 ± 0.24 mg/g, which is higher than that of the microbial strains powders alone. This suggests that adding macroporous resin to the microbial strains synergised adsorbing ginkgolic acid from the ginkgo kernel juice. Combining the two components enhanced the overall adsorption capacity, indicating that the lactic acid fermentation and macroporous resin adsorption worked together to reduce toxic ginkgolic acid in the ginkgo kernel juice more effectively.

Adsorption isotherm

Figure 6b shows the isotherm curves for ginkgolic acid adsorption at 30 °C. The experimental data were well-fitted to the Langmuir model, and the parameters obtained from the Langmuir model are listed in Supplementary Table S6. According to the Langmuir mode, the adsorption amount of ginkgolic acid C15:1 increases with increasing equilibrium concentration of ginkgolic acid in the liquid phase. At any given equilibrium

concentration of ginkgolic acid C15:1, the adsorption amount for macroporous resin was consistently the highest among the three adsorbents tested. This is followed by the mixture of resin and microbial strains, and the lowest adsorption amount was observed for the microbial debris. These results further support the conclusion drawn from the kinetic data, indicating that macroporous resin is more efficient in adsorbing ginkgolic acid than microbial strains. It is worth noting that while the Langmuir model provides a good fit for the experimental data, it is considered an empirical model with limited physical information about the mass transfer^[27]. Nonetheless, the Langmuir model offers a useful representation of the relationship between adsorption capacity and ginkgolic acid concentration in the liquid phase, and this relationship is employed in the subsequent numerical simulation.

Characterisation of microbial strains powders, macroporous resin, and their mixture before and after adsorption by FT-IR and Zeta potential

Figure 7 presents the FT-IR spectra of microbial strains powders, macroporous resin, and their mixture before and after ginkgolic acid C15:1 adsorption and ginkgolic acid C15:1 standard. The characteristic peaks in the spectra provide valuable information about the molecular composition and interactions of these components. The FT-IR spectrum of ginkgolic acid C15:1 shows distinctive peaks at specific wavenumbers. These peaks include: $3,449\text{ cm}^{-1}$, which represents the presence of -OH groups; $2,932\text{ cm}^{-1}$, indicating the presence of -C-H bonds; $1,646\text{ cm}^{-1}$, indicating the presence of C=C bonds; $1,451\text{ cm}^{-1}$, representing the characteristic peaks of a benzene ring; and $1,051\text{ cm}^{-1}$, indicating the presence of C-O bonds^[56,57]. For microbial debris, the FT-IR spectrum reveals fewer characteristic peaks, including: $2,932\text{ cm}^{-1}$, indicating the presence of -C-H bonds; $1,680\text{ cm}^{-1}$, indicating the presence of C=C bonds; and $1,447\text{ cm}^{-1}$, representing -CH₃ groups^[58,59]. In the FT-IR spectra of macroporous resin, the characteristic peaks include: $2,933\text{ cm}^{-1}$, indicating the presence of -C-H bonds; $1,606\text{ cm}^{-1}$ and $1,454\text{ cm}^{-1}$, representing the characteristic peaks of a benzene ring^[21]. After the adsorption of ginkgolic acid C15:1, the FT-IR spectra of microbial debris and the mixture of macroporous resin and microbial debris showed noticeable changes. Specifically, the peaks at $2,932\text{ cm}^{-1}$ and $1,663\text{ cm}^{-1}$ in these spectra became more intense. Also, the bands between $1,077\text{ cm}^{-1}$ and 923 cm^{-1} were strengthened in both spectra. These changes in the FT-IR spectra indicate that there are interactions between ginkgolic acid C15:1 and the microbial debris, as well as the mixture of macroporous resin and microbial debris, after the adsorption of ginkgolic acid C15:1. After adsorption, a prominent peak around $3,343\text{ cm}^{-1}$ becomes evident in the FT-IR spectra of microbial debris, macroporous resin, and their mixture. This peak indicates the presence of hydrogen bonding. It is suggested that the adsorption of ginkgolic acid C15:1 by *L. plantarum* Y2, macroporous resin, and their mixture occurs through interactions involving hydrogen bonds. Specifically, the hydroxyl groups of the adsorbent (microbial debris and macroporous resin) may form hydrogen bonds with the phenol hydroxyl groups of the adsorbate (ginkgolic acid C15:1)^[21,60].

Figure 8 presents the zeta potentials of ginkgolic acid C15:1 solution before and after adsorption. Prior to adsorption, ginkgolic acid C15:1 solution, microbial strains, macroporous resin, and the mixture of microbial strains and resin all exhibited negative charges, with zeta potential values of $-19.97 \pm$

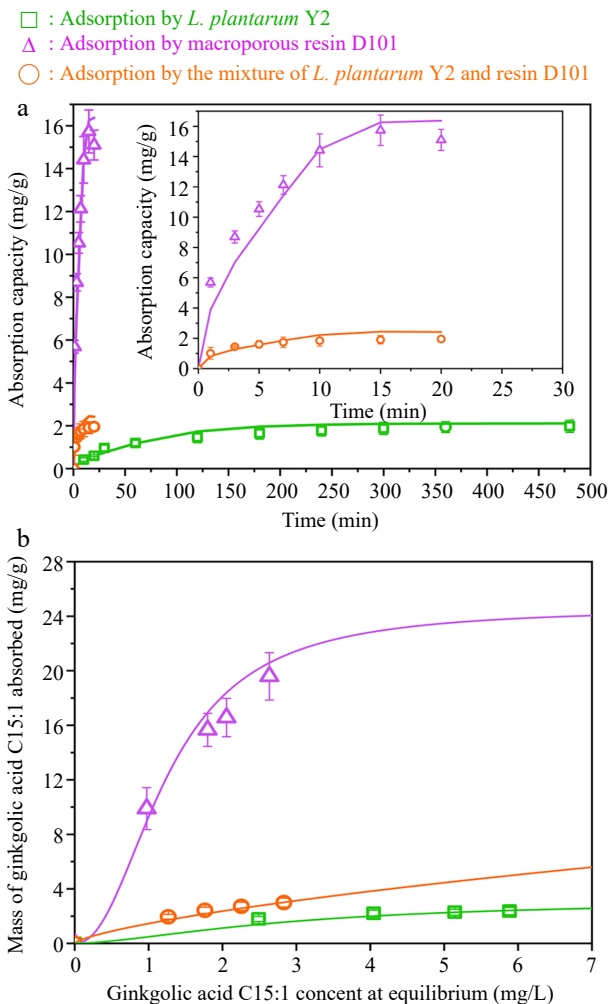


Fig. 6 (a) Experimental and simulated adsorption kinetic curves and (b) adsorption isotherms of ginkgolic acid C15:1 by different adsorbents. The points represent the experimental data, and the solid lines represent the simulated results.

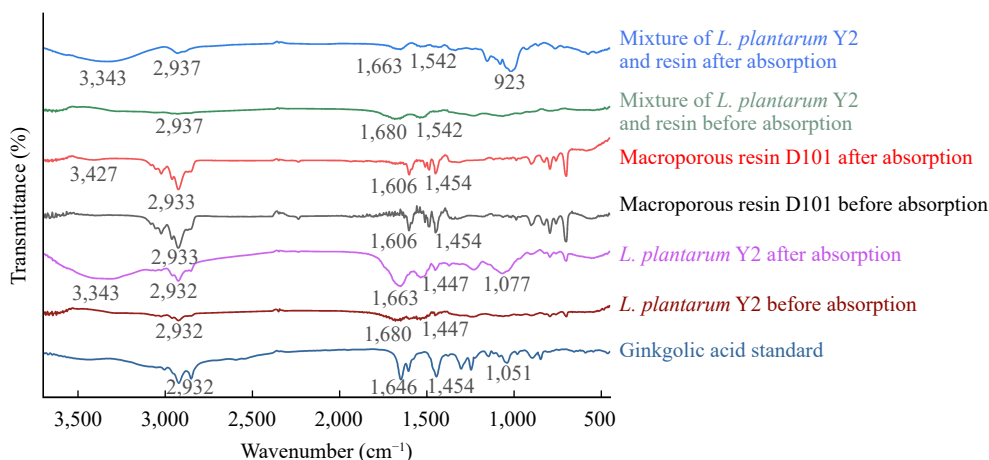


Fig. 7 FT-IR spectra of *L. plantarum* Y2, macroporous resin D101, and their mixture before and after the adsorption of ginkgolic acid C15:1.

2.00 mV, 13.93 ± 0.75 mV, 14.63 ± 0.71 mV, and -20.70 ± 0.95 mV, respectively. Following the adsorption process, the zeta potential values for ginkgolic acid C15:1 solution containing microbial strains, macroporous resin and the mixture changed. The zeta potential values were transferred to -17.80 ± 1.25 mV for the ginkgolic acid C15:1 solution with microbial strains, -14.40 ± 1.78 mV for the ginkgolic acid C15:1 solution with macroporous resin, -14.0 ± 1.15 mV for the ginkgolic acid C15:1 solution with the mixture of microbial strains and resin. The negative charges in the adsorption dispersions decreased after adsorption took place. This decline in negative charges can be attributed to the possibility of positive charge formation, given that both the adsorbents and adsorbates carried negative charges initially. The FTIR result supports this deduction, as it indicates the formation of hydrogen bonds with positive charges.

Mass transfer modeling

The physical adsorption mechanisms of ginkgolic acid C15:1 by *L. plantarum* Y2, macroporous resin, and their mixture were further examined using PVSDM modeling. Before the numerical simulation, the mass transfer parameters (k_L , D_{AB} , D_{ep}) at 30 °C were calculated and presented in Table 1. The external mass transfer rate constants (k_L) for adsorption by the microbial strains, resin, and their mixture are 6.70×10^{-9} , 6.74×10^{-6} , and 6.97×10^{-7} m/s, respectively. These data indicate that ginkgolic acid is most challenging to diffuse through the film interface between *L. plantarum* Y2 and the bulk liquid. However, adding macroporous resin to the adsorption dispersion helps alleviate the external mass transfer resistance. The higher k_L value observed for the macroporous resin can be attributed to its porous structure, which provides a large specific external surface area and more available binding sites^[61]. The D_{AB} value for ginkgolic acid C15:1 remains constant at 5.57×10^{-10} m²/s regardless of the adsorbent used. Within *L. plantarum* Y2, the D_{ep} value for ginkgolic acid C15:1 is 0 m²/s due to the solid structure of this biological material. On the other hand, the D_{ep} values within the macroporous resin and the mixture of resin and microbial strains were calculated at 8.22×10^{-11} and 1.23×10^{-11} m²/s, respectively. When considering the mixture of resin and microbial strains as an independent type of adsorbent, the integration of microbial strains weakened the diffusivity of ginkgolic acid C15:1 within the solution in the porous space of the adsorbent. In general, the addition of microbial strains

reduced the porosity of the adsorbent-containing resin and microbial strains, consequently increasing the mass transfer resistance related to pore volume diffusion. As indicated earlier, microbial strains impeded the external mass transfer of ginkgolic acid C15:1 across the solid-liquid interface, further reducing the D_{ep} value.

By utilising the above k_L , D_{AB} , and D_{ep} values, the PVSDM model successfully simulated the adsorption of ginkgolic acid C15:1 by different adsorbents. The simulation results showed satisfactory accuracy (Fig. 6a). The AAD values (lower than 15%) and R^2 values (higher than 0.9) presented in Table 1 demonstrate the excellent predictive capability of the PVSDM model. The D_s values of ginkgolic acid C15:1 obtained from PVSDM modeling are 2.51×10^{-14} , 1.67×10^{-12} , and 5.03×10^{-14} m²/s for the adsorptions by *L. plantarum* Y2, macroporous resin D101, and their mixture, respectively. As expected, ginkgolic acid C15:1 exhibited the highest D_s value within the macroporous resin, indicating relatively faster diffusion in this

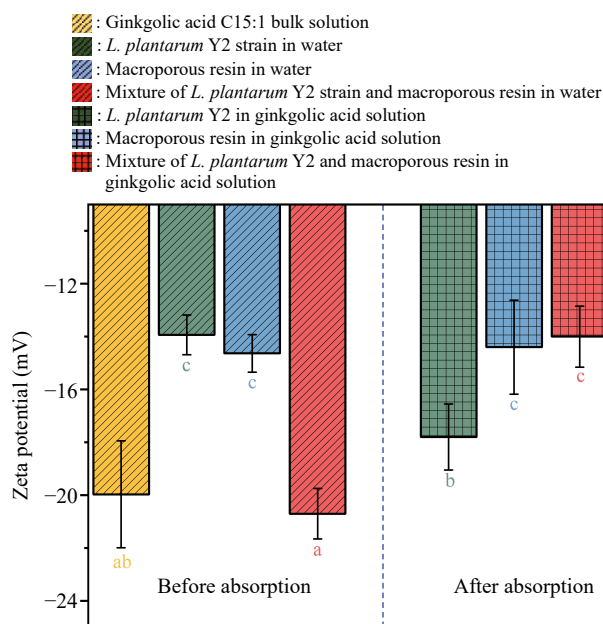


Fig. 8 Zeta potential values of the dispersions of *L. plantarum* Y2, macroporous resin, and their mixture before and after the adsorption of ginkgolic acid C15:1.

Table 1. Mass transfer parameters obtained from the PVSDM model for simulating the adsorptions of ginkgolic acid C15:1 by *L. plantarum* Y2, macroporous resin, and their mixture.

Adsorbent	k_L (m/s)	D_{AB} (m ² /s)	D_{ep} (m ² /s)	D_s (m ² /s)	AAD (%)	R ²
<i>L. plantarum</i> Y2	6.70×10^{-9}	5.57×10^{-10}	n.s.	2.51×10^{-14}	8.78	0.975
Macroporous resin D101	6.74×10^{-6}	5.57×10^{-10}	8.22×10^{-11}	1.67×10^{-12}	10.16	0.947
Mixture of <i>L. plantarum</i> and resin	6.97×10^{-7}	5.57×10^{-10}	1.23×10^{-11}	5.03×10^{-14}	13.27	0.933

n.s. refers to no pore volume diffusion.

adsorbent. Conversely, it faced the most difficulty diffusing within *L. plantarum* Y2, as reflected by the lowest D_s value. Based on these findings, it can be inferred that adding macroporous resin to the ginkgo kernel juice proved to be more effective in removing ginkgolic acids compared to the probiotic fermentation of the same juice. In our previous studies, we found that the diffusivity of blueberry phenolics within waste yeast was also lower (1.01×10^{-14} m²/s) than when they were in the framework of macroporous resin (8.50×10^{-14} m²/s)^[39]. Generally, biological adsorbents tend to create higher mass transfer resistance than resin adsorbents during the adsorption treatment. The energy theory can further explain the diffusion process alongside the solid framework of the adsorbent. Initially, ginkgolic acid molecules are adsorbed in places with high adsorption energy, providing the adsorbate with enough energy to move along the surface. Subsequently, these molecules would have enough energy to migrate to areas within the adsorbent matrix with lower adsorption energy^[62].

Since the PVSDM model assumes a spherical geometry for *L. plantarum* Y2 and treats the mixture of microbial strains and macroporous resin as a whole, it is not suitable for directly visualising the diffusional movement of ginkgolic acid within the three different adsorbents. However, despite this limitation, the PVSDM model is still capable of predicting the changes in ginkgolic acid content in the solution (Supplementary Fig. S5). This predictive capability becomes valuable in controlling the adsorption behavior during probiotic fermentation of ginkgo kernel juice, both with and without the addition of resin, in practical applications. By considering the mixture of *L. plantarum* Y2 and resin as an individual adsorbent, the mass fluxes related to pore volume diffusion (N_{AP}) and surface diffusion (N_{AS}) at the surface ($r = R$) and center ($r = 0$ m) of the three adsorbents during their adsorption of ginkgolic acid C15:1 were calculated (Supplementary Fig. S6). Throughout all three adsorption processes, both diffusion fluxes at the surface of the adsorbents decreased with time. Conversely, the values of N_{AP} and N_{AS} at the center began to increase once ginkgolic acid C15:1 diffused to the center area. After reaching their peak, N_{AP} and N_{AS} values at the center gradually declined, eventually approaching zero. The concentration/mass gradient of ginkgolic acid within the adsorbent dictated the interior mass fluxes of ginkgolic acid^[21]

Figure 9 illustrates the contributions of surface diffusion to the overall intraparticle diffusion (SDCP%) at the surface ($r = R$) and center ($r = 0$ m) of each adsorbent during the adsorption of ginkgolic acid. For the adsorption of ginkgolic acid by *L. plantarum* Y2, the SDCP% value remains at 100% throughout since there is no pore volume diffusion in the solid adsorbent. On the other hand, in the adsorption of ginkgolic acid by the macroporous resin, surface diffusion contributed less to the intraparticle diffusion than pore volume diffusion. The SDCP% values during adsorption ranged from 24.1% to 31.1%. These data

suggest that ginkgolic acid is primarily adsorbed by the resin through diffusion along the interior pores of the material. This finding is reasonable because there is less mass transfer resistance for the diffusion of ginkgolic acid in the liquids within the resin pores than the diffusion alongside the solid resin framework.

The mass transfer behavior during the adsorption process involving the microbial strains and resin mixture showed distinct differences compared to the adsorption by each individual adsorbent. Incorporating macroporous resin into the suspension reduced the contribution of surface diffusion to the overall diffusion, particularly when compared with the adsorption by *L. plantarum* Y2. The SDCP% value at the adsorbent surface decreased below 65% in the mixed adsorbent suspension. The changing pattern of the SDCP% value for each adsorption treatment suggests that adding macroporous resin to the suspension containing the microbial strains creates a more porous area for the adsorption of ginkgolic acid. This, in turn, alleviates the mass transfer resistance for surface diffusion and

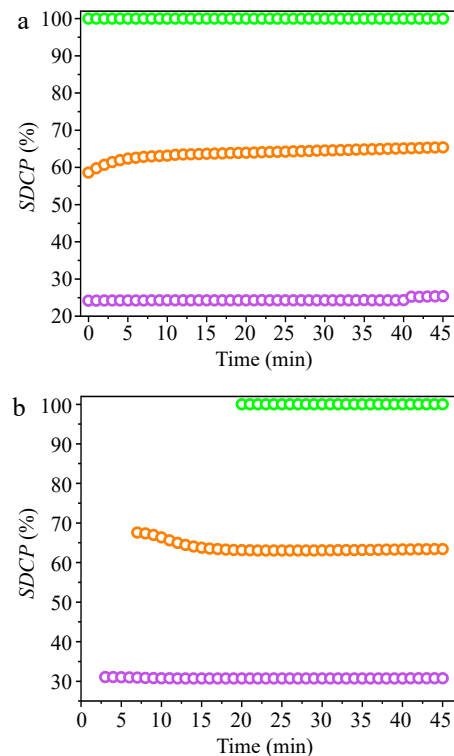


Fig. 9 SDCP% values at various times and different radial positions within the adsorbents, representing the contribution of surface diffusion to the overall intraparticle diffusion (green: *L. plantarum* Y2; purple: macroporous resin D101; orange: the mixture of *L. plantarum* and resin, where the combination was treated as a unified entity). (a) SDCP at the surface of each adsorbent ($r = R$). (b) SDCP at the center of each adsorbent ($r = 0$).

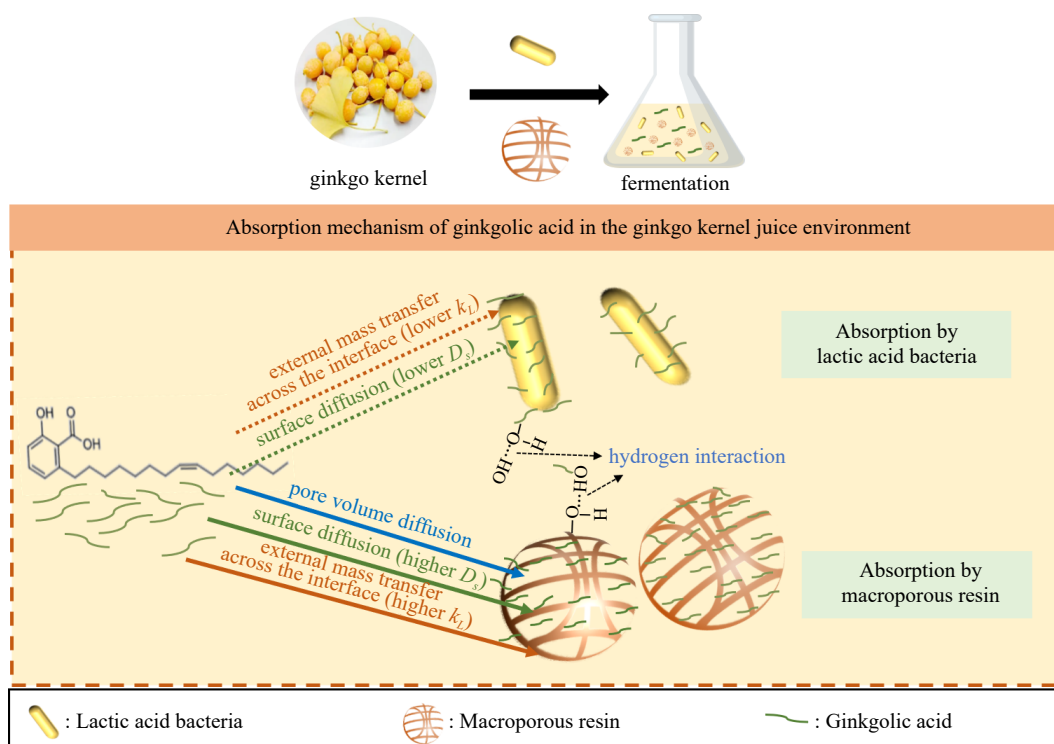


Fig. 10 The schematic of adsorption of ginkgolic acid by microbial strains, macroporous resin and their mixture.

consequently enhances the overall adsorption efficiency and the amount of toxic ginkgolic acid removed.

Conclusions

The presence of toxic components in ginkgo kernels hinders consumer acceptance, putting significant pressure on *Ginkgo biloba* tree plantations and the environment. However, this study presents a novel and environmentally friendly approach for effectively removing these toxic components from ginkgo kernel juice through lactic acid fermentation with the addition of macroporous resin. The results demonstrated that using isolated lactic acid bacteria in the presence of macroporous resin led to the removal of over 69% of ginkgolic acid C13:0 and ginkgolic acid C15:1, and over 61% of MPN from the ginkgo kernel juice. This removal of toxic constituents surpassed the efficacy of techniques reported in the existing literature. Furthermore, a significant finding was made during this study, revealing that the adsorption of microbial growth inhibitors, such as ginkgolic acid and phenolics, by the resin did not impact the microbial growth and metabolism of organic acids and monosaccharides during probiotic fermentation. This study also established mass transfer theories for the adsorption of ginkgolic acid by microbial strains, with and without the addition of macroporous resin. Generally, the microbial adsorption process involves the diffusion of ginkgolic acid within the solid structure of microbial strains. The incorporation of macroporous resin introduced the element of pore volume diffusion to the adsorption of ginkgolic acid, enhancing the removal of toxic components during the probiotic fermentation of ginkgo kernel juice (Fig. 10). This study presents a promising and effective method for detoxifying ginkgo kernel juice, contributing to environmentally friendly and safe food processing.

Overall, this study presents a comprehensive and systemic approach, offering a green technique to remove toxic constituents from ginkgo kernel juice. This exploration and the establishment of scientific theories further support the effectiveness of this detoxification method. Ultimately, this work addresses safety concerns and boosts consumer confidence in ginkgo kernel products.

Author contributions

The authors confirm contribution to the paper as follows: study conception: Tao Y, Han Y; investigation: Sun Y, Zhao J, He J, Tao Y; methodology: Sun Y, Zhao J, He J, Li D; validation: Sun Y, Tao Y; draft manuscript preparation & Formal analysis: Sun Y; data curation: Tao Y; manuscript review & editing: Manickam S, Li D, Han Y, Jiang X, Tao Y; supervision: Han Y, Jiang X; funding acquisition: Tao Y. All authors reviewed the results and approved the final version of the manuscript.

Data availability

All data generated or analyzed during this study are included in this published article.

Acknowledgments

This work was supported by Jiangsu Key Research and Development Program - Modern Agriculture (BE2021353), National Natural Science Foundation of China (No. 32072351), Fundamental Research Funds for the Central Universities, China (No. YDZX2023017), Jiangsu Agricultural Science and Technology Independent Innovation Fund (No. CX(22)2026) and Jiangsu University Qinglan Project.

Conflict of interest

The authors declare that they have no conflict of interest.

Supplementary Information accompanies this paper at (<https://www.maxapress.com/article/doi/10.48130/FIA-2023-0032>)

Dates

Received 10 October 2023; Accepted 14 December 2023; Published online 28 December 2023

References

1. Major RT. 1967. The Ginkgo, the most ancient living tree: The resistance of *Ginkgo biloba* L. to pests accounts in part for the longevity of this species. *Science* 157:1270–73
2. van Beek TA. 2005. Ginkgolides and bilobalide: Their physical, chromatographic and spectroscopic properties. *Bioorganic & Medicinal Chemistry* 13(17):5001–12
3. Zhou G, Yao X, Tang Y, Qian D, Su S, et al. 2014. An optimized ultrasound-assisted extraction and simultaneous quantification of 26 characteristic components with four structure types in functional foods from ginkgo seeds. *Food Chemistry* 15(1):177–85
4. Boateng ID, Zhang W, Li Y, Saalia FK, Yang X. 2021. Non-thermal pretreatment affects *Ginkgo biloba* L. seed's product qualities, sensory, and physicochemical properties. *Journal of Food Science* 12:94–111
5. Wang H, Shi M, Cao F, Su E. 2022. *Ginkgo biloba* seed exocarp: A waste resource with abundant active substances and other components for potential applications. *Food Research International* 160:111637
6. Ahlemeyer B, Krieglstein J. 2003. Neuroprotective effects of *Ginkgo biloba* extract. *Cellular and Molecular Life Sciences CMLS* 60:1779–92
7. Jang HS, Roh SY, Jeong EH, Kim BS, Sunwoo MK. 2015. Ginkgotoxin Induced Seizure Caused by Vitamin B6 Deficiency. *Journal of Epilepsy Research* 5(2):104–6
8. Kobayashi D, Yoshimura T, Johno A, Sasaki K, Wada K. 2011. Toxicity of 4'-O-methylpyridoxine-5'-glucoside in *Ginkgo biloba* seeds. *Food Chemistry* 126(3):1198–202
9. Fan GJ, Wang X, Wu CE, Pan HM, Yang JT, et al. 2017. Effect of heating on the content and composition of ginkgolic acids in ginkgo seeds. *Quality Assurance and Safety of Crops & Foods* 9(2):195–99
10. Lim HB, Kim DH. 2018. Effects of roasting conditions on physicochemical properties and antioxidant activities in *Ginkgo biloba* seeds. *Food Science and Biotechnology* 27(4):1057–66
11. Liu J, Chen J, Ye S, Ding Y, Guo S, et al. 2023. Inhibitory action of ginkgolic acid against pathogenic fungi and characterisation of its inhibitory activities on *Nigrospora oryzae*. *Folia Horticulturae* 35:49–59
12. Wang Y, Tao Y, Zhang X, Shao S, Han Y, et al. 2019. Metabolic profile of ginkgo kernel juice fermented with lactic acid bacteria: A potential way to degrade ginkgolic acids and enrich terpene lactones and phenolics. *Process Biochemistry* 76:25–33
13. Hathout AS, Aly SE. 2014. Biological detoxification of mycotoxins: a review. *Annals of Microbiology* 64(3):905–19
14. Delcour J, Ferain T, Deghorain M, Palumbo E, Hols P. 1999. The biosynthesis and functionality of the cell-wall of lactic acid bacteria. *Antonie van Leeuwenhoek* 76:159–84
15. Bueno DJ, Casale CH, Pizzolitto RP, Salvano MA, Oliver G. 2007. Physical adsorption of aflatoxin B₁ by lactic acid bacteria and *Saccharomyces cerevisiae*: A theoretical model. *Journal of Food Protection* 70:2148–54
16. Ge N, Xu J, Peng B, Pan S. 2017. Adsorption mechanism of tenuazonic acid using inactivated lactic acid bacteria. *Food Control* 82:274–82
17. Zhang W, Zou M, Wu R, Jiang H, Cao F, et al. 2021. Efficient removal of ginkgotoxin from *Ginkgo biloba* seed powder by combining endogenous enzymatic hydrolysis with resin adsorption. *Journal of the Science of Food and Agriculture* 101:1589–97
18. Kou Z, Wang C. 2022. Preparation of polyhydroxyl adsorbent and its application in the removal of Ginkgolic acids. *Industrial Crops and Products* 184:114998
19. Estevinho L, Paula AP, Moreira L, Dias LG, Pereira E. 2008. Antioxidant and antimicrobial effects of phenolic compounds extracts of Northeast Portugal honey. *Food and Chemical Toxicology* 46:3774–79
20. Li S, Tao Y, Li D, Wen G, Zhou J, et al. 2021. Fermentation of blueberry juices using autochthonous lactic acid bacteria isolated from fruit environment: Fermentation characteristics and evolution of phenolic profiles. *Chemosphere* 276(1):130090
21. Wu Y, Han Y, Tao Y, Fan S, Chu D, et al. 2018. Ultrasound assisted adsorption and desorption of blueberry anthocyanins using macroporous resins. *Ultrasonics Sonochemistry* 48:311–20
22. Balestra GM, Misaghi IJ. 1997. Increasing the efficiency of the plate counting method for estimating bacterial diversity. *Journal of Microbiological Methods* 30(2):111–17
23. Wu Y, Li S, Tao Y, Li D, Han Y, et al. 2021. Fermentation of blueberry and blackberry juices using *Lactobacillus plantarum*, *Streptococcus thermophilus* and *Bifidobacterium bifidum*: Growth of probiotics, metabolism of phenolics, antioxidant capacity in vitro and sensory evaluation. *Food Chemistry* 348:129083
24. Gong W, Zhao X, Manickam S, Liu X, Li D, et al. 2023. Impact of cell wall adsorption behaviours on phenolic stability under air drying of blackberry with and without contact ultrasound assistance. *Food Hydrocolloids* 137(1):108312
25. Zou M, Zhang W, Wu R, Jiang H, Cao F, et al. 2021. Removal of ginkgotoxin from the *Ginkgo biloba* seeds powder by adopting membrane separation technology. *Journal of Cleaner Production* 280:124452
26. Wu Y, Han Y, Tao Y, Li D, Xie G, et al. 2020. In vitro gastrointestinal digestion and fecal fermentation reveal the effect of different encapsulation materials on the release, degradation and modulation of gut microbiota of blueberry anthocyanin extract. *Food Research International* 132:109098
27. Tao Y, Wu P, Dai Y, Luo X, Manickam S, et al. 2022. Bridge between mass transfer behavior and properties of bubbles under two-stage ultrasound-assisted physisorption of polyphenols using macroporous resin. *Chemical Engineering Journal* 436(1):135158
28. Franco DSP, Vieillard J, Salau NPG, Dotto GL. 2020. Interpretations on the mechanism of In(III) adsorption onto chitosan and chitin: A mass transfer model approach. *Journal of Molecular Liquids* 304:112758
29. Leyva-Ramos R, Geankoplis CJ. 1985. Model simulation and analysis of surface diffusion of liquids in porous solids. *Chemical Engineering Science* 40:799–807
30. Ocampo-Perez R, Leyva-Ramos R, Alonso-Davila P, Rivera-Utrilla J, Sánchez-Polo M. 2010. Modeling adsorption rate of pyridine onto granular activated carbon. *Chemical Engineering Journal* 165:133–41
31. Leyva-Ramos R, Ocampo-Perez R, Mendoza-Barron J. 2012. External mass transfer and hindered diffusion of organic compounds in the adsorption on activated carbon cloth. *Chemical Engineering Journal* 183:141–51
32. Podstawczyk D, Witek-Krowiak A. 2016. Novel nanoparticles modified composite eco-adsorbents—a deep insight into kinetics modelling using numerical surface diffusion and artificial neural network models. *Chemical Engineering Research and Design* 109:1–17

Detoxification of ginkgo kernel juice

33. Pauletto PS, Moreno-Pérez J, Hernández-Hernández LE, Bonilla-Petriciolet A, Dotto GL, et al. 2021. Novel biochar and hydrochar for the adsorption of 2-nitrophenol from aqueous solutions: An approach using the PVSDM model. *Chemosphere* 269:128748
34. Fröhlich AC, Ocampo-Pérez R, Díaz-Blancas V, Salau NPG, Dotto GL. 2018. Three dimensional mass transfer modeling of ibuprofen adsorption on activated carbon prepared by sonication. *Chemical Engineering Journal* 341:65–74
35. Ocampo-Pérez R, Rivera-Utrilla J, Gómez-Pacheco C, Sánchez-Polo M, López-Peñalver JJ. 2012. Kinetic study of tetracycline adsorption on sludge-derived adsorbents in aqueous phase. *Chemical Engineering Journal* 213:88–96
36. Valderrama C, Gamisans X, De las Heras X, Farrán A, Cortina JL. 2008. Sorption kinetics of polycyclic aromatic hydrocarbons removal using granular activated carbon: intraparticle diffusion coefficients. *Journal of Hazardous Materials* 157:386–96
37. Wilke CR, Chang P. 1955. Correlation of diffusion coefficients in dilute solutions. *AIChE Journal* 1:264–70
38. Furusawa T, Smith JM. 1973. Fluid-particle and intraparticle mass transport rates in slurries. *Industrial & Engineering Chemistry Fundamentals* 12:197–203
39. Tao Y, Wu Y, Han Y, Chemat F, Li D, et al. 2020. Insight into mass transfer during ultrasound-enhanced adsorption/desorption of blueberry anthocyanins on macroporous resins by numerical simulation considering ultrasonic influence on resin properties. *Chemical Engineering Journal* 380(1):122530
40. Souza PR, Dotto GL, Salau NPG. 2017. Detailed numerical solution of pore volume and surface diffusion model in adsorption systems. *Chemical Engineering Research and Design* 122:298–307
41. Xia Y, DeBolt S, Dreyer J, Scott D, Williams MA. 2015. Characterization of culturable bacterial endophytes and their capacity to promote plant growth from plants grown using organic or conventional practices. *Frontiers in Plant Science* 6:490
42. Liao W, Shen J, Manickam S, Li S, Tao Y, et al. 2023. Investigation of blueberry juice fermentation by mixed probiotic strains: Regression modeling, machine learning optimization and comparison with fermentation by single strain in the phenolic and volatile profiles. *Food Chemistry* 405:134982
43. Park JJ, Lee WY. 2021. Adsorption and desorption characteristics of a phenolic compound from *Ecklonia cava* on macroporous resin. *Food Chemistry* 338:128150
44. Zhou G, Ma J, Tang Y, Wang X, Zhang J, et al. 2018. Multi-response optimization of ultrasonic assisted enzymatic extraction followed by macroporous resin purification for maximal recovery of flavonoids and ginkgolides from waste *Ginkgo biloba* fallen leaves. *Molecules* 23:1029
45. Boateng ID. 2022. A critical review of ginkgolides in *Ginkgo biloba* leaf extract (EGb): toxicity and technologies to remove ginkgolides and their promising bioactivities. *Food & Function* 18:9226–42
46. Qian Y, Peng Y, Shang E, Zhao M, Yan L, et al. 2017. Metabolic profiling of the hepatotoxicity and nephrotoxicity of Ginkgolides in rats using ultra-performance liquid chromatography-high-definition mass spectrometry. *Chemico-Biological Interactions* 273:11–17
47. Chinese Association of Integrative Medicine, Chinese Medical Doctor Association, National Clinical Research Center for Chinese Medicine Cardiology, Cardiovascular Disease Working Group, Encephalopathy Disease Working Group, et al. 2021. Chinese expert consensus on clinical application of oral *Ginkgo biloba* preparations (2020). *Chinese Journal of Integrative Medicine* 27(3):163–69
48. European Pharmacopoeia Commission. 2010. *Monograph: Ginkgo dry extract. Refined and quantified*. European Directorate for the Quality of Medicines & Healthcare, Strasbourg, France.
49. United States Pharmacopeia. 2010. *Thirty-Fourth Revision: Powdered Ginkgo Extract*. The United States Pharmacopoeial Convention, Rockville, Md, US.
50. Dong Q, Cao J, Wu R, Shi T, Zhang W, et al. 2021. Efficient removal of ginkgolides from *Ginkgo biloba* leaves crude extract by using hydrophobic deep eutectic solvents. *Industrial Crops and Products* 166:113462
51. Hong SJ, Jang JA, Hwang H, Cho MS. 2017. Changes in 4'-O-methylpyridoxine (ginkgotoxin) and antioxidant activity in ginkgo biloba seeds in different cooking conditions. *Korean Journal of Food Science and Technology* 49(5):532–37
52. Zou M, Zhang W, Dong Q, Tang C, Cao F, et al. 2021. Submerged fermentation of *Ginkgo biloba* seed powder using *Eurotium cristatum* for the development of ginkgo seeds fermented products. *Journal of the Science of Food and Agriculture* 101(5):1782–91
53. Leonard W, Zhang P, Ying D, Adhikari B, Fang Z. 2021. Fermentation transforms the phenolic profiles and bioactivities of plant-based foods. *Biotechnology Advances* 49:107763
54. García-Ruiz A, Cueva C, González-Rompinelli EM, Yuste M, Torres M, et al. 2012. Antimicrobial phenolic extracts able to inhibit lactic acid bacteria growth and wine malolactic fermentation. *Food Control* 28:212–19
55. Gao M, Wang D, Deng L, Liu S, Zhang K, et al. 2021. High-crystallinity covalent organic framework synthesized in deep eutectic solvent: Potentially effective adsorbents alternative to macroporous resin for flavonoids. *Chemistry of Materials* 33:8036–51
56. Chen HY, Ting Y, Kuo HC, Hsieh CW, Hsu HY, et al. 2021. Enzymatic degradation of ginkgolides by laccase immobilized on core/shell Fe₃O₄/nylon composite nanoparticles using novel coaxial electrospinning process. *International Journal of Biological Macromolecules* 172:270–80
57. Boateng ID, Yang XM, Li YY. 2021. Optimization of infrared-drying parameters for *Ginkgo biloba* L. seed and evaluation of product quality and bioactivity. *Industrial Crops and Products* 160:113108
58. Amiri S, Mokarram RR, Khiabani MS, Bari MR, Alizadeh M. 2021. Optimization of food-grade medium for co-production of bioactive substances by *Lactobacillus acidophilus* LA-5 for explaining probiotic mechanisms of probiotic. *Journal of Food Science and Technology* 58:1–12
59. Wang WQ, Zhang JL, Yu Q, Zhou JY, Lu ML, et al. 2021. Structural and compositional changes of whey protein and blueberry juice fermented using *Lactobacillus plantarum* or *Lactobacillus casei* during fermentation. *RSC Advances* 11:26291–302
60. Caglar B, Cubuk O, Demir E, Coldur F, Catir M, et al. 2015. Characterization of AlFe-pillared Unye bentonite: a study of the surface acidity and catalytic property. *Journal of Molecular Structure* 1089:59–65
61. Hernández-Padilla ES, Zárate-Guzmán AI, González-Ortega O, Padilla-Ortega E, Gómez-Durán A, et al. 2022. Elucidation of adsorption mechanisms and mass transfer controlling resistances during single and binary adsorption of caffeic and chlorogenic acids. *Environmental Science and Pollution Research* 29:26297–311
62. Ocampo-Pérez R, Leyva-Ramos R, Sanchez-Polo M, Rivera-Utrilla J. 2013. Role of pore volume and surface diffusion in the adsorption of aromatic compounds on activated carbon. *Adsorption* 19:945–57



Copyright: © 2023 by the author(s). Published by Maximum Academic Press on behalf of China Agricultural University, Zhejiang University and Shenyang Agricultural University. This article is an open access article distributed under Creative Commons Attribution License (CC BY 4.0), visit <https://creativecommons.org/licenses/by/4.0/>.